BJRS
BRAZILIAN JOURNAL OF RADIATION SCIENCES

doi.org/10.15392/2319-0612.2024.2419
2024, 12(1) | 01-33 | e2419
Submitted: 2024-01-06
Accepted: 2024-02-29

Overview of Fourth Generation Reactors Studied at the *Universidade Federal de Minas Gerais* (Brazil)

Silva [a*], C. A. M.; Macedo[a], A. A. P.; Gilbert[a], M.; Silva[a], F. C.; Magalhães[a], I. R.; Costa[a], A. L.; Pereria[a], C.

[a] Nuclear Engineering Department, Universidade Federal de Minas Gerais, Av. Antônio Carlos, 6627, Campus UFMG, PCA01, Pampulha, 31270-901, Belo Horizonte, MG

*clarysson@nuclear.ufmg.br

Abstract: This paper presents the results of the studies about the Fourth Generation Reactors developed at DENU-UFMG, such as the Very High Temperature Reactor (VHTR), Molten Salt Breeder Reactor (MSBR), Sodium Fast Reactor (SFR) and Gas-cooled Fast Reactor (GFR). These studies evaluate neutronic parameters of the nuclear system at steady state and during the burnup using computer models developed at DENU-UFMG using SCALE 6.0 (KENO-VI/ORIGENS), MCNPX 2.6.0 and MCNP5. The results show that the adopted methodologies confirm the capabilities of the codes to simulate specific situations in steady state or transient operating conditions.

Keywords: Generation Four Nuclear Reactors, Nuclear Fuel Cycle, Neutronic simulations.

BJRS
BRAZILIAN JOURNAL OF RADIATION SCIENCES

doi.org/10.15392/2319-0612.2024.2419
2024, 12(1) | 01-33 | e2419
Submitted: 2024-01-06
Accepted: 2024-02-29

Panorama dos Estudos sobre Reatores de Quarta Geração Realizados na Universidade Federal de Minas Gerais (Brasil)

Resumo: Este artigo apresenta resultados dos estudos sobre reatores de quarta geração desenvolvidos no Departamento de Engenharia Nuclear da Universidade Federal de Minas Gerais (DENU-UFMG), tais como o Reator refrigerado a Gás de Alta Temperatura (VHTR), Reator Regenerador a Sal Fundido (MSBR), Reator Rápido refrigerado de Sódio (SFR) e Reator Rápido Refrigerado a Gás (GFR). Esses estudos avaliam parâmetros neutrônicos dos sistemas nucleares em estado estacionário e durante a queima utilizando modelos computacionais desenvolvidos no DENU-UFMG utilizando o códigos SCALE 6.0 (KENO-VI/ORIGENS), MCNPX 2.6.0 e MCNP5. Os resultados mostram que as metodologias adotadas confirmam as capacidades dos códigos para simular situações específicas em condições de operação estacionária ou transiente.

Palavras-chave: Reatores de Quarta Geração, Ciclo do Combustível Nuclear, Simulação Neutrônica.

SBPR

1. INTRODUCTION

The demand projections of the global energy show an increasing trend and require greater use of reliable energy sources. Nuclear power plants may represent very attractive options for energy generation because of its high compliance degree with sustainability criteria and its high capacity factor compared to other energy alternatives [1]. However, there are still economics, proliferation, safety, and waste production issues that innovative approaches should enhance. The new generation of nuclear systems presents advanced concepts that may break out of the limitations of currently used nuclear energy systems. The Fourth Generation Reactors offer potential benefits, including possible lower costs, enhanced safety, greater resource utilization, waste minimization, co-production of process heat for industrial operations, improved proliferation resistance, and easier operation [2].

In the last decades, several researches have been developed around the world where the "International Project on Innovative Nuclear Reactors and Fuel Cycles" (INPRO) and the "Generation IV Forum" (GIF) are important initiatives concerning the discussions on the future of nuclear reactor technology. Formally, Brazil participates of INPRO and was also involved in GIF until recently. For better efforts coordination of Brazilian researchers and aiming at increase the importance and visibility of Brazil in the international forums on innovative and advanced nuclear systems, the "National Institute for Advanced and Innovative Nuclear Reactors (INCT-RNI)" was created in 2008 [3]. This institute has as mission to perform research and prepare human resources for developing innovative nuclear reactor technologies for the sustainable development of Brazil.

Among the scientific institutions that compose the INCT-RNI is the Nuclear Engineering Department of the Universidade Federal de Minas Gerais (DENU-UFMG), which has been studying advanced nuclear systems. The research group of DENU-UFMG

has as a goal evaluates the innovative fuel cycle associated with neutronic analysis of the new reactor generation, as it is presented in this paper. The reactors VHTR, MSBR, GFR, and SFR have been simulated by nuclear codes as SCALE 6.0 (KENO-VI/ORIGENS), MCNPX 2.6.0 and MCNP5 (e.g. [4-26]). These nuclear systems will tend to have closed fuel cycles and transmute the long-lived actinides: they are expected to have full actinide recycling. In this way, the present paper overviews the simulated systems, and the results are discussed as follows.

2. USED CODES

Monte Carlo (MC) codes have been widely used around the world to simulate the neutronic behavior of different nuclear reactors. The SCALE 6.0 and MCNPX 2.6.0 are mostly MC codes used to analyze steady-state neutronic parameters such as the multiplication factor, neutron flux, reaction rate, reactor physics constants, and time dependent burnup calculations. The steady-state analyses are performed by particle transport calculus using MC method. This technique plays a relevant role to perform the neutronic calculation over the spatial dependence of the neutron flux in fully three-dimensional geometry. On the other hand, the time dependent calculation is a linked process that involves the steady-state results with the nuclide depletion that is performed by an external module, for example, SCALE 6.0 uses KENO-VI coupling with ORIGENS to burnup calculations, while MCNPX 2.6.0 uses MCNP coupling with CINDER-90 module. These coupled calculations aim to predict the temporal changes in the core's material composition and neutronic parameters changes. However, stochastic codes present a larger computational cost than deterministic methods, mainly due to geometry details. This characteristic implicates to the enormous computational time in the burnup calculation. In this work, the steady-state simulations are performed before the time dependent calculation to optimize the computational time. This methodology was employed in MHR, GFR and SFR systems. In

the MSBR, the coolant/fuel (molten salt) flows through the reactor core and it is subjected to continuous reprocessing. The MCNPX 2.6.0 and SCALE 6.0 do not comprise this continuous reprocessing in the fuel depletion calculation which is different of other types of nuclear systems. Thus, the MSBR study presents analysis only at steady-state aims and evaluates the fuel composition for future burnup calculation studies.

In the present work, the MCNPX2.6.0 and SCALE6.0 use the ENDF-B-VII.0 library. The MCNPX uses this library as a continuous one, and the SCALE6.0 code uses 238 groups collapsed from the ENDF-B-VII.0 continuous library (V7-238).

3. SIMULATED SYSTEMS

3.1. Very High Temperature Reactor

Gas-cooled reactors have been investigated since the early days of nuclear power. The early gas reactors were used commercially in the United Kingdom [27] but were overshadowed by the Light Water Reactors (LWR) and other designs. Recently, interest in gas-cooled reactors has been renewed, and several High Temperature Gas Reactor (HTGR) designs have been developed for near-term deployment. The VHTR concept is an evolutionary extension beyond the near term HTGR designs. The VHTR is a helium-cooled, graphite-moderated reactor with a ceramic core and TRISO coated fuel particles, where the fissile fuel is enclosed within layers of temperature resistant materials, including SiC and pyrolytic graphite. These particles are compacted with graphite powder to form the fuel pins inserted into hexagonal fuel assemblies. The reactor core consists of an array of hexagonal graphite blocks distributed in three regions: inner ring, central ring and outer ring. The reflector blocks are placed into inner and external rings. The fuel assemblies and the control rods blocks are arranged into the central ring [28]. This geometry was modeled in the MCNP5 code (Figure 1) where the core design was based on previous studies [29].

Figure 1: VHTR core simulated by MCNP5

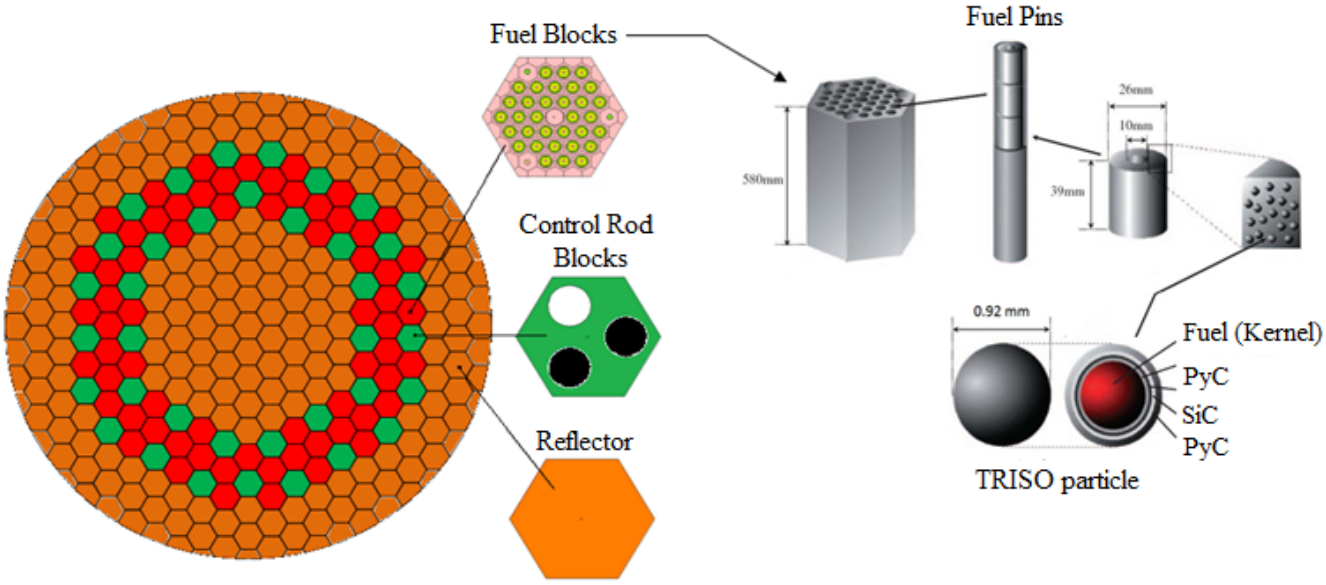

Firstly, two models were evaluated to verify the geometry sensitivity in the simulations: heterogeneous (HE) and semi-homogeneous (SH). The HE model simulates the TRISO particles geometries and compositions. In the SH model, the TRISOs were not simulated but the particles densities and the compositions were homogenized into fuel pins. Table 1 presents the effective multiplication factor (k_{eff}) of the VHTR core for HE and SH models and for the reference case (RC) [29] with UO_2 fuel enriched at 15%. Figure 2 depicts the MCNP5 modeling for both the HE and SH cases.

Table 1: The k_{eff} of Reference Case (RC) and simulated models SH and HE

MODEL	k_{eff}	STANDARD DEVIATION
RC [29]	1.35484	0.00119
SH	1.35545	0.00045
HE	1.35545	0.00045

Figure 2: Heterogeneous (HE) and Semi-Homogeneous (SH) models.

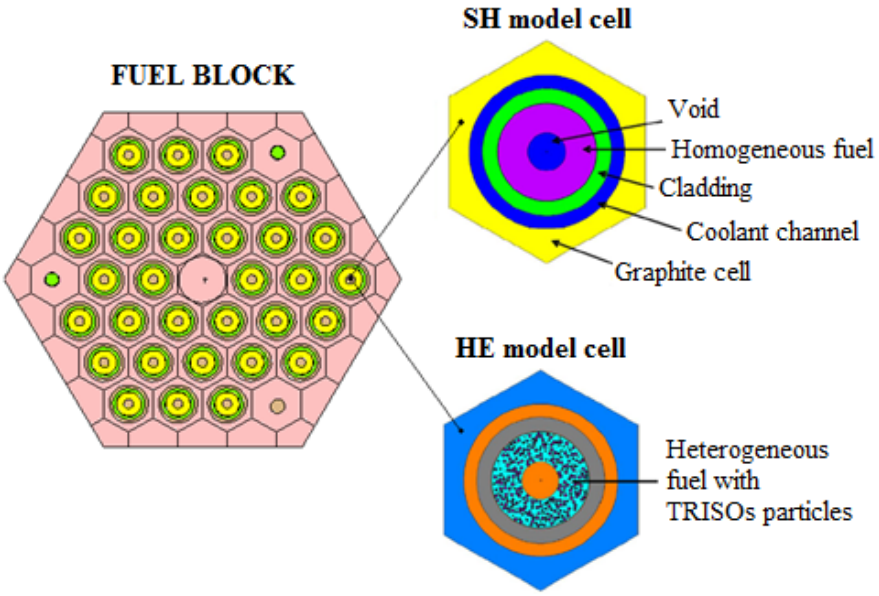

Among the cases, the results of RC and SH have the most considerable similarity. The difference of k_{eff} between them is 61.0 pcm, and considering the standard deviation, the k_{eff} of these models is statistically equal. On the other hand, between RC and HE model, this difference is 719 pcm. Thus, the SH model has a more significant agreement with the RC than the HE model because the SH model uses the same homogenization methodology than RC case. Despite of the differences, the models have similar k_{eff} values and to save computational time, the SH model can be used in the neutronic studies.

In VHTR concept, it is inevitable that the quantity of TRISO particles into fuel pins has a fundamental role in the reactor performance. Different packing fraction (PF) of TRISO particles associated with different fissile content (FC) in the fuel, generates unlike behavior of neutronic parameters. In order to evaluate keff and neutron flux as functions of PF and FC, several PF-FC combinations were simulated using the SH model. Two fuel types were simulated: (a) enriched uranium (EU), and (b) a mix of depleted uranium and reprocessed plutonium (U-Pu). Figures 3 and 4 illustrate the k_{eff} values to EU and U-Pu respectively. In these figures, each curve represents a FC percentage in the fuel, where keff values increase as FC rises. Also, for a same FC value, the keff values increase as PF rises because the fuel

volume is proportional to PF. As PF rises, the volume of fissile material increases and contributes to k_{eff} rise. As the total volume of fuel pin does not change, this PF increasing represents an increase in the TRISO particle volume, but a reduction in the graphite volume (moderator), which generates a hardening in the neutron flux.

Figure 3: Effective multiplication factor as function PF-FE to EU fuel type

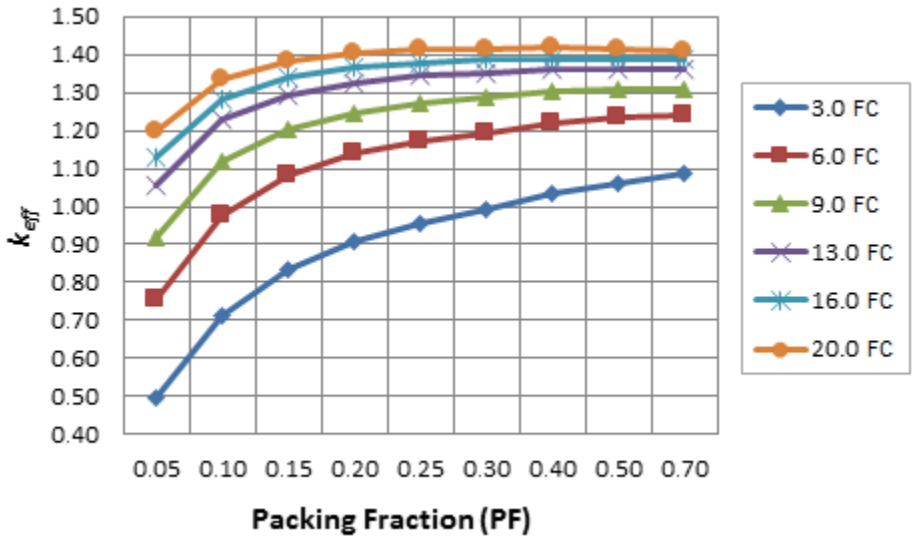

Figure 4: Effective multiplication factor as function PF-FE to U-Pu fuel type

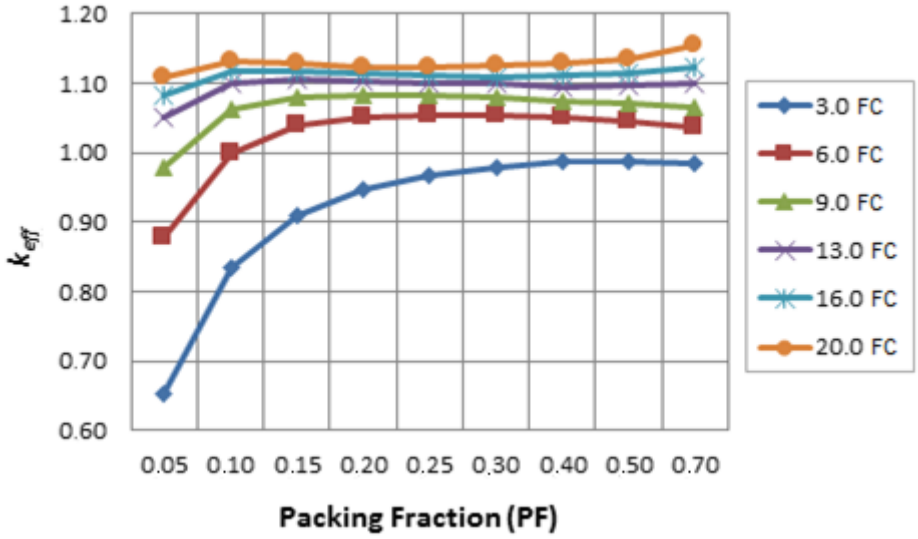

Figure 5: Fast to total neutron flux ratio into fuel pin (EU fuel type)

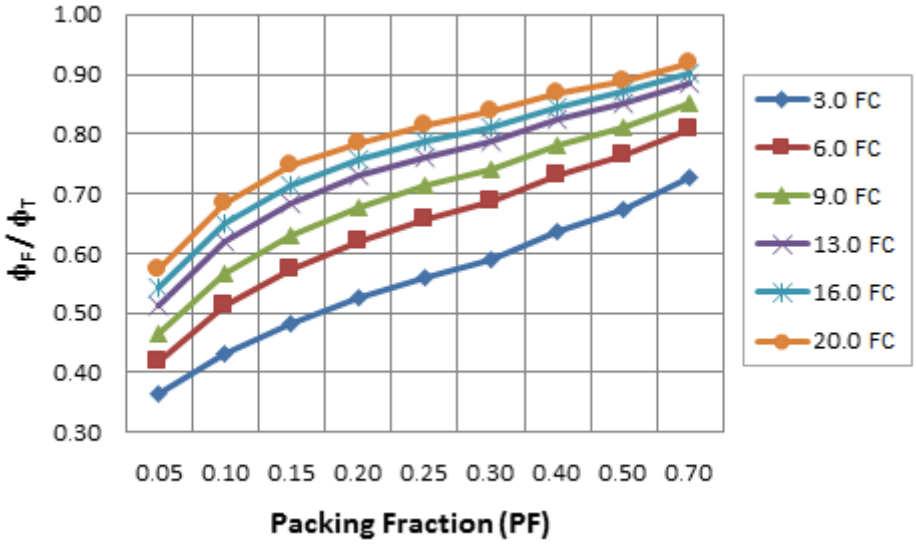

Figure 6: Fast to total neutron flux ratio into fuel pin (U-Pu fuel type)

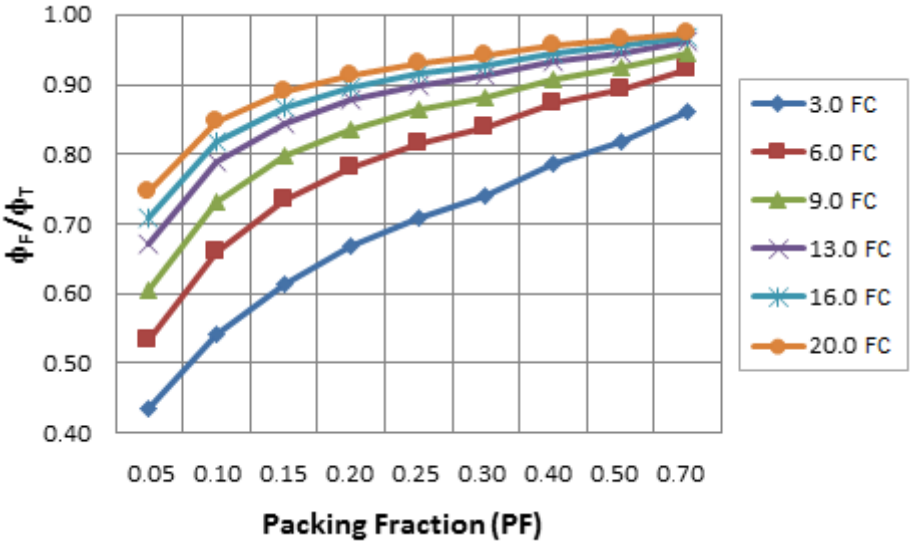

Figures 5 and 6 illustrate the fast to total neutron flux ratio (ϕ_F/ϕ_T) inside the fuel pin to both simulated fuels. The ϕ_F/ϕ_T increases as PF increases for all simulated cases. Considering that the fission probability to fissile isotopes is higher to thermal neutrons, a hardening neutron spectrum may reduce the fission reaction number. This behavior may contribute to stabilizing k_{eff} values as PF increases. This tendency is more remarkable in the

highest FC values (Figure 3 and 4), because of the increase in the hardening neutron spectrum of these cases (Figure 5 and 6). The k_{eff} and ϕ_F/ϕ_T present similar values to FC = 13.0, 16.0 and 20.0, with the smallest difference being PF ≥ 0.30.

Between the two fuel types, for the same PF-FC value, the U-Pu has smallest k_{eff} and the most hardened neutron spectrum. This behavior may be due to Pu isotopes, which have high probability of radiative capture reaction for thermal neutrons.

Based on reference value, the burnup study considers FC=16.0 among the evaluated cases. As verified, the smallest and the highest FC values generate the smallest and the highest k_{eff} respectively. Thus, the fuel depletion analysis regard to intermediate PF value (0.30). The simulations consider 1,000 days at hot full power with specific power density of 103 W/g. Figure 7 depicts k_{eff} values during the irradiation cycle of VHTR to EU and U-Pu fuels.

Figure 7: Effective multiplication factor as a function of burnup

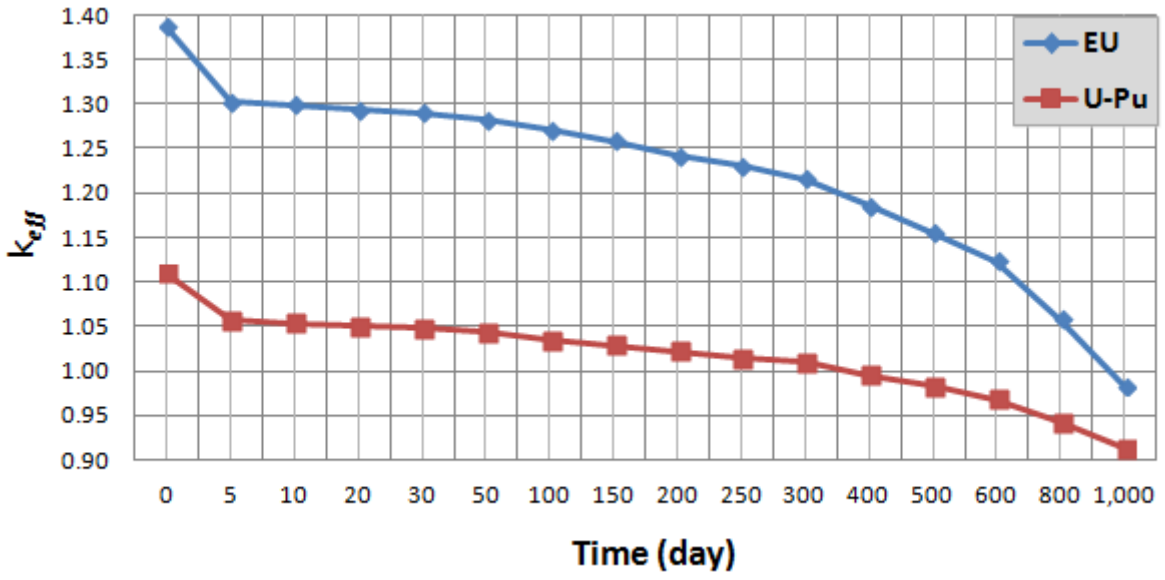

The simulations consider 1,000 days at full power with a specific power density of 103 MWD/MTU. As expected, the k_{eff} reduces during the burnup, but between the two fuel types, the k_{eff} variation is 0.404 to EU and 0.197 to U-Pu. Thus, U-Pu has the half in keff reduction between the two fuel types compared to EU. Both fuels have the same FC and

PF; this behavior can be due to the presence of neutron absorbers in U-Pu, at BOL. The presence these nuclides may reduce the initial k_{eff}, but its gradual transmutation during the burnup, may generate a smoother k_{eff} reduction to U-Pu compared to EU. Therefore, between the evaluated fuels, the results may indicate less use of neutron absorber during the burnup to U-Pu fuel.

Table 2 presents the isotopic mass of the evaluated fuels at Beginning of Life (BOL), and End Of Life (EOL), and Figures 8 and 9 illustrate the mass variation (Δm (%)) between BOL and EOL, which was calculated regarding to total fuel mass.

Table 2: Isotopic mass (g) and mass variation (Δm) between BOL and EOL

NUCLIDE	EU				U-Pu			
	BOL	**EOL**	**Δm**	**Δm(%)**	**BOL**	**EOL**	**Δm**	**Δm(%)**
^{234}U	0.00E+00	1.19E+00	1.19E+00	2.39E-04	0.00E+00	4.20E+01	4.20E+01	8.41E-03
^{235}U	7.91E+04	2.38E+04	-5.53E+04	-1.11E+01	7.50E+02	4.10E+02	-3.40E+02	-6.80E-02
^{236}U	0.00E+00	9.14E+03	9.14E+03	1.83E+00	0.00E+00	7.79E+01	7.79E+01	1.56E-02
^{237}U	0.00E+00	1.23E+01	1.23E+01	2.47E-03	0.00E+00	2.51E-01	2.51E-01	5.02E-05
^{238}U	4.21E+05	4.06E+05	-1.50E+04	-3.00E+00	3.79E+05	3.63E+05	-1.57E+04	-3.14E+00
^{239}U	0.00E+00	4.08E-01	4.08E-01	8.16E-05	0.00E+00	3.88E-01	3.88E-01	7.76E-05
^{237}Np	0.00E+00	5.13E+02	5.13E+02	1.03E-01	0.00E+00	1.70E+01	1.70E+01	3.39E-03
^{238}Np	0.00E+00	1.25E+00	1.25E+00	2.50E-04	0.00E+00	2.72E-02	2.72E-02	5.44E-06
^{239}Np	0.00E+00	5.88E+01	5.88E+01	1.18E-02	0.00E+00	5.59E+01	5.59E+01	1.12E-02
^{238}Pu	0.00E+00	1.15E+02	1.15E+02	2.30E-02	2.80E+03	2.24E+03	-5.65E+02	-1.13E-01
^{239}Pu	0.00E+00	4.33E+03	4.33E+03	8.67E-01	7.35E+04	2.93E+04	-4.42E+04	-8.85E+00
^{240}Pu	0.00E+00	1.32E+03	1.32E+03	2.65E-01	3.14E+04	2.73E+04	-4.07E+03	-8.14E-01
^{241}Pu	0.00E+00	8.97E+02	8.97E+02	1.79E-01	5.93E+03	1.32E+04	7.30E+03	1.46E+00
^{242}Pu	0.00E+00	2.86E+02	2.86E+02	5.72E-02	6.49E+03	8.00E+03	1.51E+03	3.02E-01
^{243}Pu	—	—	—	—	0.00E+00	9.30E-01	9.30E-01	1.86E-04
^{244}Pu	—	—	—	—	0.00E+00	2.19E-01	2.19E-01	4.38E-05
^{241}Am	—	—	—	—	0.00E+00	8.18E+02	8.18E+02	1.64E-01
^{242}Am	—	—	—	—	0.00E+00	5.65E+00	5.65E+00	1.13E-03
^{243}Am	—	—	—	—	0.00E+00	1.58E+03	1.58E+03	3.16E-01
^{244}Am	—	—	—	—	0.00E+00	8.81E-01	8.81E-01	1.76E-04
^{242}Cm	—	—	—	—	0.00E+00	1.74E+02	1.74E+02	3.47E-02
^{243}Cm	—	—	—	—	0.00E+00	4.64E+00	4.64E+00	9.28E-04
^{244}Cm	—	—	—	—	0.00E+00	8.71E+02	8.71E+02	1.74E-01
^{245}Cm	—	—	—	—	0.00E+00	6.52E+01	6.52E+01	1.30E-02
^{246}Cm	—	—	—	—	0.00E+00	4.82E+00	4.82E+00	9.64E-04

Figure 8: Variation in U and Pu mass between BOL and EOL

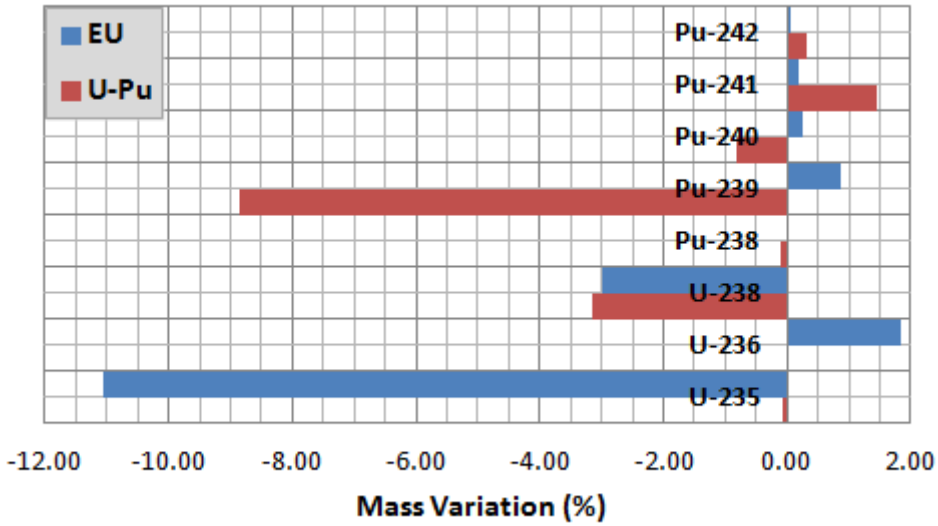

Figure 9: Variation in Cm, Am and Np mass between BOL and EOL

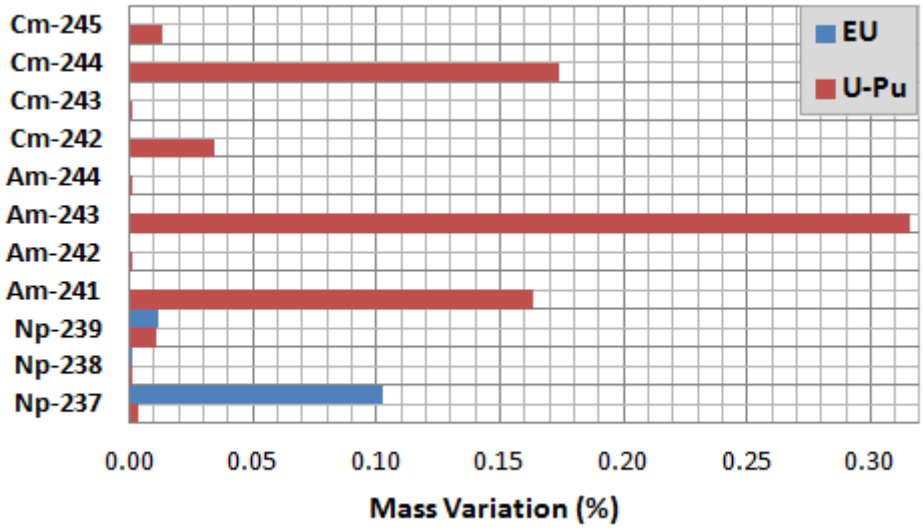

Between the two fuel types, the mass of ^{238}Pu, ^{239}Pu and ^{240}Pu reduce to U-Pu but increase to EU. Among these nuclides, the more expressive difference is to ^{239}Pu, were the U-Pu fuel presents a reduction of 8.8% and EU increase of 0.8% in ^{239}Pu mass (Figure 8). This behavior is due to the fission of 239Pu in U-Pu and the transmutation of ^{238}U in ^{239}Pu

in EU. Also, the mass of Np is smallest to U-Pu fuel. Among the Np isotopes, the ^{237}Np presents the biggest difference (Figure 9) where the production this nuclide is higher to EU fuel. The ^{237}Np is formed through the consecutives reactions

$$^{235}\text{U}(n,\gamma) \rightarrow {}^{236}\text{U}\ (n,\gamma) \rightarrow {}^{237}\text{U}\ (\beta^{-}) \rightarrow {}^{237}\text{Np}.$$

Thus, as the EU has higher ^{235}U mass at BOL (Table 2), the concentration of 237Np is higher to this fuel type.

However, the U-Pu presents an increase of the ^{243}Pu, ^{244}Pu, Am and Cm, while the EU do not have these isotopes in its final composition (Table 2). Among these nuclides, the increase of ^{241}Am, ^{243}Am, ^{244}Cm and ^{242}Cm are more evident (Figure 9). This behavior may be due the presence of Pu in the U-Pu fuel where the beta decay of ^{241}Pu and ^{243}Pu produce ^{241}Am and ^{243}Am, respectively. Also, during the reactor cycle there is production ^{242}Am and ^{244}Am, which decay to ^{242}Cm and ^{244}Cm, respectively.

Therefore, concerning to reprocessed U-Pu fuel, the simulations present a reduction of Pu mass but an increase of Np, Am and Cm mass (Table 3) where the reduction of Pu is higher than the production of Np, Am, and Cm.

Table 3: Total mass variation (Δm(%)) between BOL and EOL by chemical element type

FUEL TYPE	ELEMENT				
	U	Np	Pu	Am	Cm
EU	-1.22E+01	1.15E-01	1.39E+00	0.00E+00	0.00E+00
U-Pu	-3.19E+00	1.46E-02	-8.01E+00	4.81E-01	2.24E-01

3.2. Molten Salt Breeder Reactor

This reactor concept was developed in the 1960s by Oak Ridge National Laboratory (ORNL), which was operated successfully demonstrated high burnup and on-line fueling [30]. Today the Molten Salt Reactor is one of the promising future nuclear reactor concepts included in the Generation IV roadmap. In this nuclear system, the fuel is a circulating

mixture of salts between the reactor core and the heat exchanger. Thorium fueled MSR concept is one of the most promising nuclear reactors designs currently being studied because of the high natural availability of this fuel. The aim is use ^{232}Th to breed ^{233}U, where uranium (^{233}U or ^{235}U) is the initial source of fissile material that needs to be provided. However, plutonium (Pu) and minor actinides (MAs) could be used instead of uranium for initial fissile loading. In this sense, the MCNPX 2.6.0 code was used to calculate the criticality and the neutron flux profile at the steady state of MSBR core. The MSBR configurations use the data from a conceptual design developed by ORNL [31]. Figure 10 illustrates the geometry of the simulated system, where graphite is the main material other than salt which is used for neutron moderation and reflection. The reactor core has a square lattice that contains graphite blocks with a square cross section and a circular fuel channel.

Figure 10: Model of the MSBR simulated in MCNPX 2.6.0

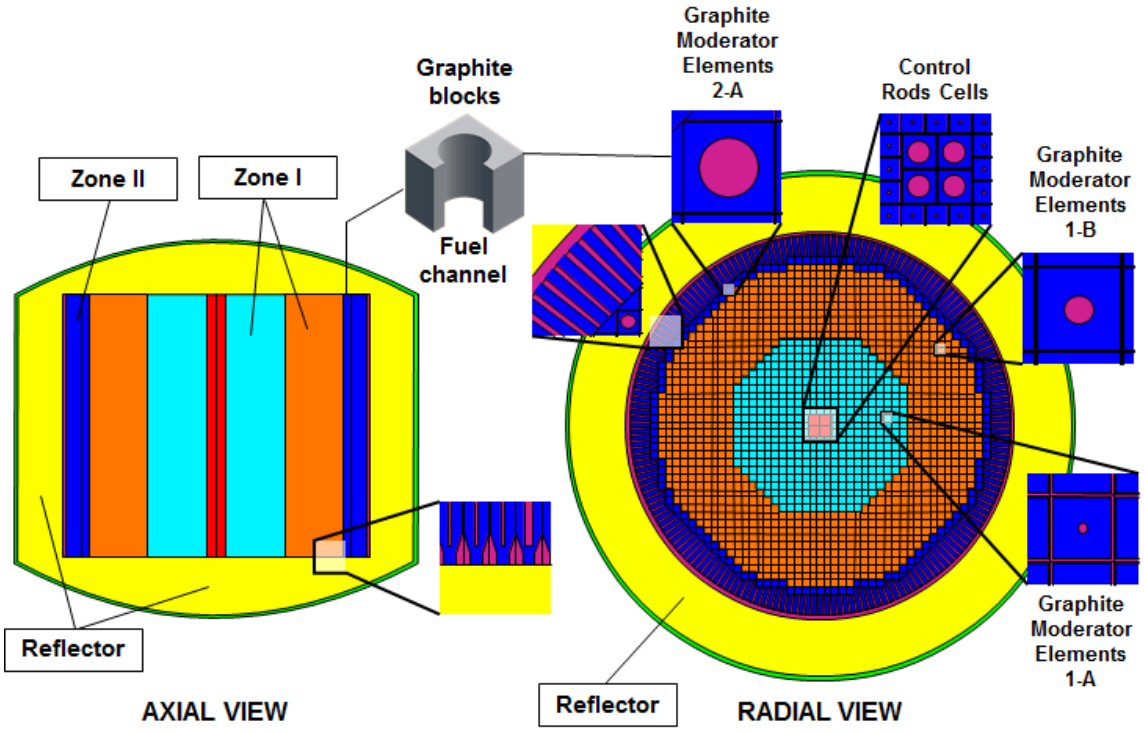

Firstly, the MCNPX model was compared to previous studies considering the conventional ^{233}U (^{232}Th fuel with 1.76% fissile content [32, 33]. Table 4 presents the

effective multiplication factor (k_{eff}) at beginning of cycle (BOC) of the MSBR system simulated by DENU-UFMG (this work), University of Illinois at Urbana-Champaign (UIUC) [32], Ulsan National Institute of Science and Technology (UNIST) [33] and Korea Atomic Energy Research Institute (KAERI) [33]. In the present study, the calculated k_{eff} by the MCNPX 2.6.0 code agrees with others works. The highest difference is related to the SERPENT code. According to reference [32], this discrepancy may be due to the simplifications in Zone II performed in the SERPENT model.

Table 4: MSBR criticality at BOC to RU fuel calculated by different institutes

UNIVERSITY/INSTITUTE	USED CODES	k_{eff}	DIFF (pcm)
DENU/UFMG	MCNPX 2.6.0	1.01010	—
UIUC [32]	MCNP6	1.00736	274.0
	SERPENT	1.00389	621.0
UNIST & KAERI [33]	MCNP6	1.01277	267.0

In the second step, different nuclides were evaluated as an initial seed of the system in the fission/transmutation process. Thus, the following fuel types were simulated:

1) Recovery Uranium (RU): Conventional ^{233}U from the U-Th cycle;
2) Enriched Uranium (EU): ^{235}U manufactured by enrichment plant;
3) Reprocessed Plutonium (RP): Nuclides of Pu from spent PWR fuel; and
4) Reprocessed Actinides (RA): Matrix of Pu/AMs from spent PWR fuel.

Table 5 presents the k_{eff} of the MSR core for the evaluated fuels. These fuels were simulated with two fissile isotopes concentrations because the ORNL reports two values which represent a conceptual (2.26%) and an optimized (1.76%) MSBR design [31]. The results show that the same weight fraction of fissile isotopes does not produce similar k_{eff} values. This behavior can be due to: (a) the presence of nuclides in RP and RA fuels that have high neutrons cross section for radiative capture; and/or (b) the different atomic masses of the fissile isotopes, because the fuel that contains fissile isotopes with the lightest mass

has more fissile atoms. In this sense, the fissions number may be highest for the RU, producing highest k_{eff} value. Thus, increasing the concentration of fissile isotopes of RP and RA fuels is necessary, such that they have k_{eff} values similar to the RU fuel.

Table 5: Effective multiplication factor for the evaluated fuels

FISSILE ISOTOPES (% MASS)	FUEL TYPE			
	RU	EU	RP	RA
1.76	1.01010	0.89823	0.88793	0.82751
2.26	1.12413	0.99576	0.90546	0.83596

Table 6 presents k_{eff} as a function of fissile isotopes content and heavy metal concentration. As expected, k_{eff} increases as fissile isotopes augment. The k_{eff} of RP and RA are similar to RU when the mass of the fissile isotopes is 16 and 25%, respectively. Then, this percentage was used to calculate the total neutron flux in MSR core.

Table 6: Effective multiplication factor as a function of fissile isotopes

FISSILE ISOTOPES (% MASS)	HEAVY METAL (% MASS)			k_{eff}	
	Th	Pu	Pu/AMs	RP	RA
10.0	83.9	16.1	—	0.94234	0.82546
15.0	75.9	24.1	—	0.99776	—
16.0	74.3	25.7	—	1.01143	—
17.0	72.6	27.4	—	1.02497	—
18.0	71.0	29.0	—	1.03864	—
19.0	69.4	30.6	—	1.05241	—
20.0	62.7	—	37.3	—	0.94310
21.0	60.8	—	39.2	—	0.95648
22.0	59.0	—	41.0	—	0.97081
23.0	57.1	—	42.9	—	0.98452
24.0	55.2	—	44.8	—	0.99907
25.0	53.4	—	46.6	—	1.01359
26.0	51.5	—	48.5	—	1.02701

Figure 11 illustrates the radial neutron flux profile in the reactor core to RU, RP, and RA fuels. The central region (Zone I) has the highest flux, while the outer zone presents the smallest one. This behavior is expected because the simulations do not comprise the reactivity control. The peripheral region is the reflector where the neutron flux is almost zero, so there is no neutron leakage from the reactor core. For RU fuel type, the center core presents a depletion of this flux which the absence of control rods may have produced. The withdrawal of the graphite control rod inserts negative reactivity to the core due to the decrease of neutron moderation. The reprocessed fuels (RP and RA) present a neutron flux profile more flatten than RA. Although the RP and RA have a concentration of fissile isotopes higher than RU, the reprocessed fuels have neutron absorbers that may cause a neutron flux reduction. This behavior suggests that to RP and RA, a different radial distribution of the fuel blocks into MSR core is necessary to flatten the neutron flux profile.

Figure 11: Total neutron flux in the MSR core

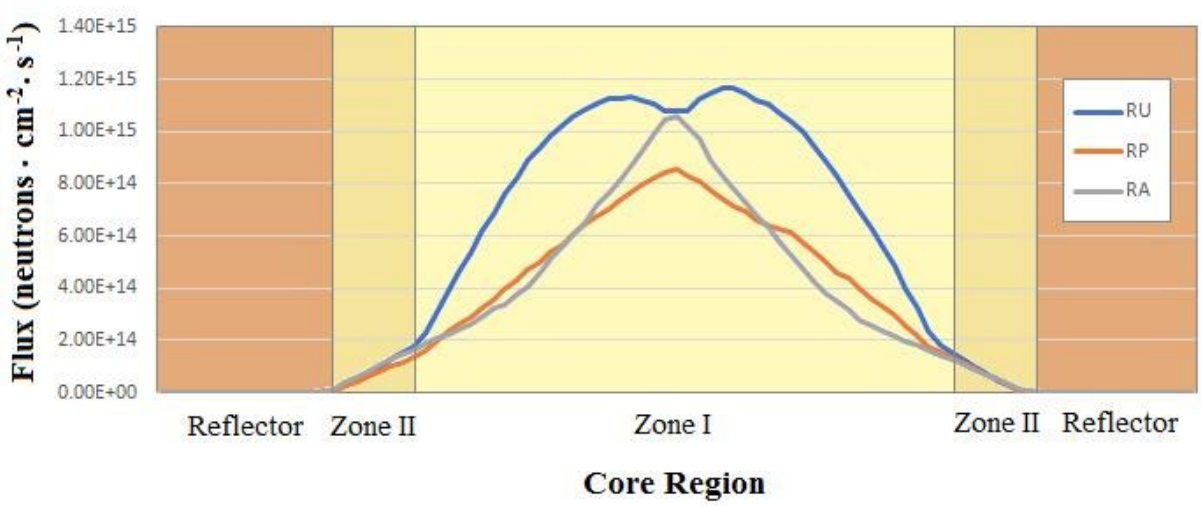

3.3. Gas Cooled Fast Reactor

The first fast breeder reactor, called Clementine, was constructed in the 1946 during the Manhattan Project at Los Alamos National Laboratory in the US. In the 1960s, prototype reactors operated in China, France, Germany, India, Japan, the Russian Federation, the

United Kingdom and the United States [34]. Although there has been stagnation in the development of fast reactors in past decades, in the countries involved, this reactor concept represents an important role in the advanced reactors. In 2002, the Generation IV International Forum (GIF) selected six nuclear system concepts to compound the fourth generation reactors list. In this role, four types are fast reactors, among which is the Gas-cooled Fast Reactor (GFR). The GFR can fully utilize fuel resources, minimize or reduce its own (and other systems) actinide inventory, produce high efficiency electricity, and utilize high temperature process heat [35]. In this way, the research group DENU-UFMG has been used the SCALE 6.0 and MCNPX 2.6.0 codes to evaluate the GFR criticality under steady state and burnup conditions. Three carbide fuel types were evaluated:

1) Natural uranium and plutonium – (U, Pu)C;
2) Depleted uranium and transuranic – (U,TRU)C; and
3) Thorium and transuranic – (Th, TRU)C

Figure 12 shows the configured model comprising the active core without the reflector layers. Thus, to minimize the lack of reflector layers, these simulations comprise reflective surface boundaries, so there are no neutron leakages. The core dimensions, geometry and properties were based in the reference work [36]. Previous studies [14,15] verified that the most suitable percent of the fissile material for each nuclear fuel is 11.33% for (U,Pu)C, 13.06% for (U,TRU)C and 15.78% for (Th,TRU)C which produce similar k_{inf} for the three fuels.

Figure 12: GFR core configuration

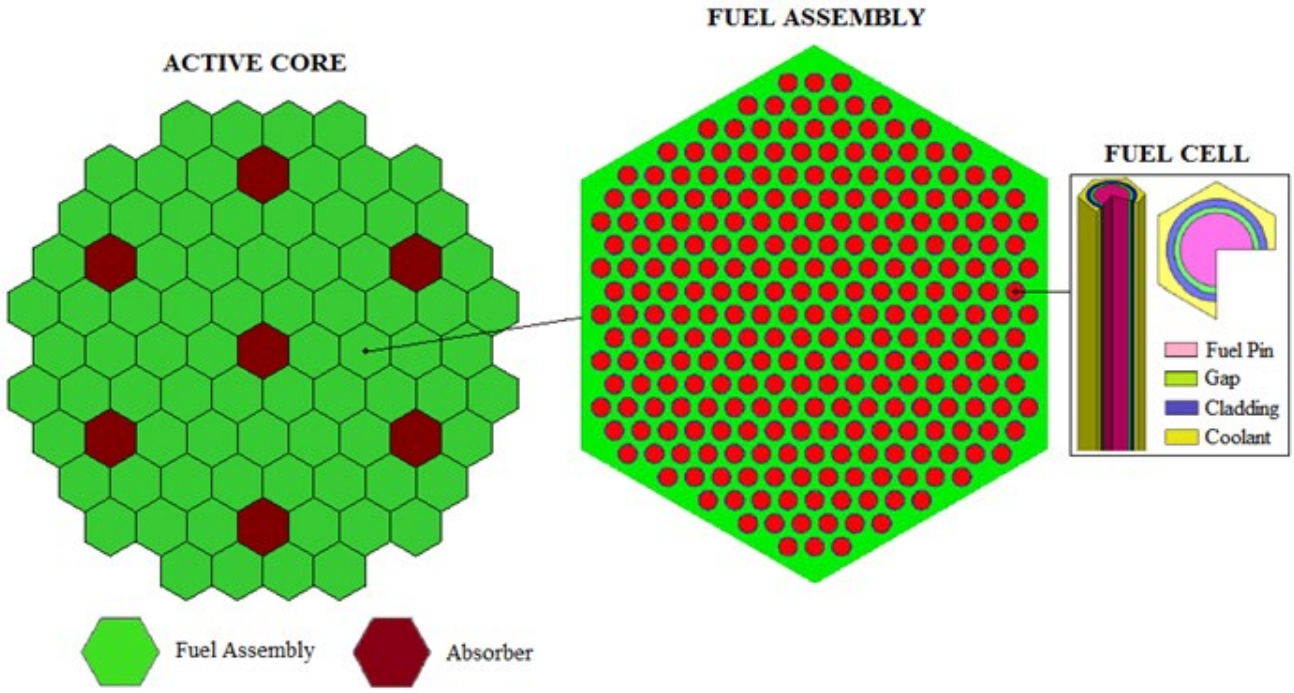

Table 7: Infinite multiplication factor at BOC and EOC considering 1400 days of burnup

FUEL COMPOSITION	(U, Pu)C		(U, TRU)C		(Th, TRU)C	
	MCNPX	SCALE	MCNPX	SCALE	MCNPX	SCALE
BOC	1.30270	1.30713	1.30039	1.30499	1.29860	1.30353
EOC	1.17824	1.17080	1.18847	1.18142	1.23279	1.22089

Table 7 presents the infinite multiplication factor (k_{inf}) at Beginning of Cycle (BOC) and End of Cycle (EOC) and the Figure13 illustrates the behavior of this factor during the burnup. In the simulations, the specific power of the GFR is 48 W/g. Between the codes, the kinf values are very similar and the small differences may be attributed to the data treatment between the codes. The MCNPX code uses a continuous library, but the SCALE6.0 code uses 238 groups collapsed from the ENDF-B-VII.0. Also, MCNPX performs the burnup using the CINDER90 code using 63 energy groups and the SCALE6.0 uses the ORIGEN-S, which performs the burnup using 3 energy groups. Among the fuels,

the (Th, TRU)C has the biggest k_{inf} at EOC, because of ^{233}U build-up effects. The (U,Pu)C and (U, TRU)C present similar k_{inf} at EOC.

Figure 13: Infinite multiplication factor as a function of time

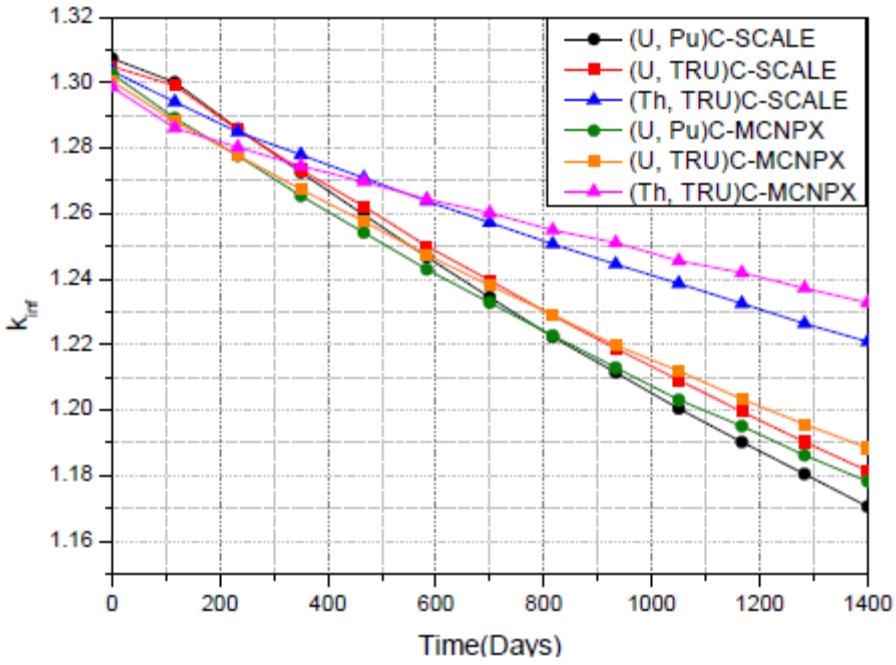

Figures 14, 15, and 16 show the variation in the atomic density of main nuclides during the burnup to (U, Pu)C, (U, TRU)C and (Th, TRU)C respectively. These variations are similar in the used codes and the results present good agreement between then. The (U, Pu)C presents an increase of ^{239}Pu and ^{241}Pu, and a decrease of ^{238}Pu (Figure 14). These behaviors can be due to the fission of ^{239}Pu and ^{241}Pu and because of the transmutation of ^{238}U in ^{238}Pu. In the (U,TRU)C fuel, there is an increase of ^{244}Cm while the ^{241}Am and ^{237}Np concentrations are practically constant (Figure 15). Regard to (U,Th)C fuel, due to the ^{232}Th transmutation, there is a buildup of ^{233}Th and ^{233}Pa, which are responsible for the ^{233}U production (Figure 16). During the burnup, there is a gradual increase of ^{233}U, but it tends to stabilize during the reactor cycle. Among the evaluated fuels, the (Th,TRU)C presents the higher generation of fissile isotopes that produce the highest k_{inf} at EOC (Figure 15).

Figure 14: Evolution of Pu isotopes in (U,Pu)C fuel during the burnup

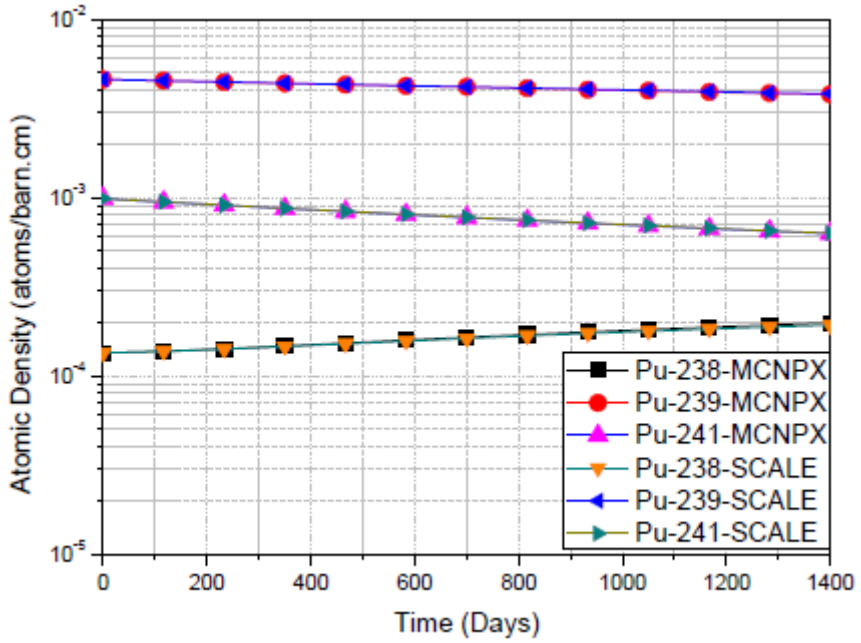

Figure 15: Evolution of Am, Cm and Np in (U,TRU)C fuel during the burnup

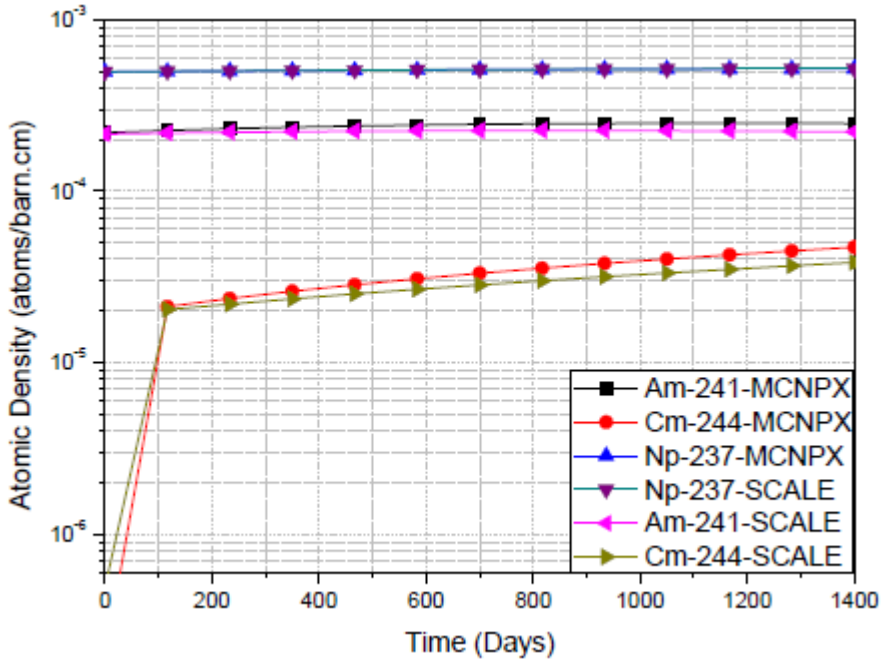

Figure 16: Evolution of ^{233}Th, ^{233}Pa and ^{233}U in (Th, TRU)C fuel during the burnup

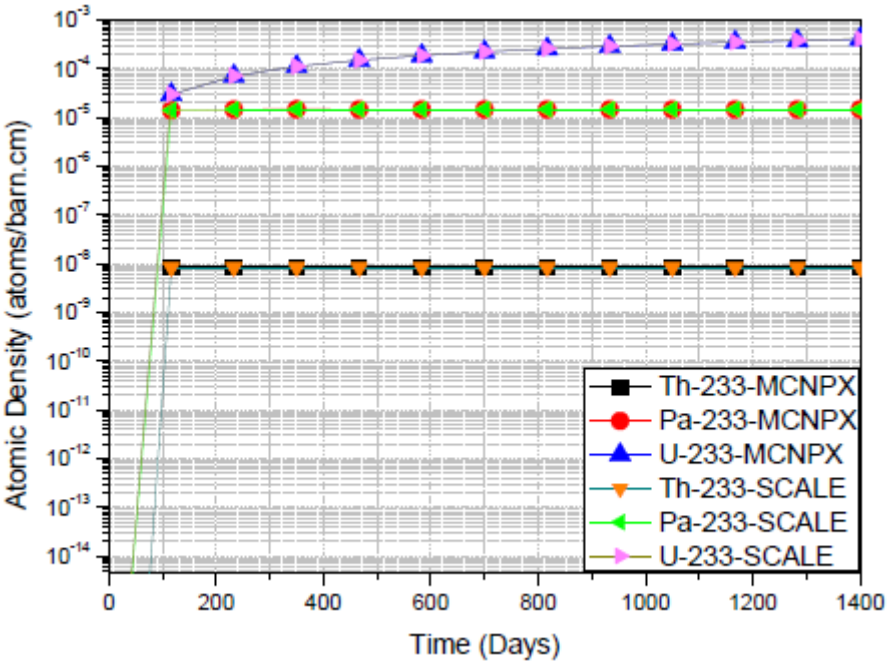

3.4. Sodium Fast Reactor

The sodium-cooled fast reactor (SFR) is one of the four fast neutron concepts selected by the GIF withsignificant industrial experience feedback. Approximately, twenty prototypes or demonstrators have been built throughout the world, which has demonstrated the excellent use of the uranium resource, as well as, the capability of these reactors to recycle the plutonium without any limitation in the number of recycling operations (multi-recycling) [37]. On the other hand, there is interest in developing small and medium sized reactors because of their attractive features as compatibility for small electricity grids; lower capital costs; reduced design complexity; among others advantages [38]. Therefore, engaging these factors, the research group DENU-UFMG has studied a small fast sodium reactor concept similar to the 4S concept from Toshiba. This reactor includes passive nuclear safety systems and does not require on-site refueling. This concept is not a breeder reactor because there is no uranium blanket around the core for the absorption of neutrons leakage, but its hardening neutron spectrum provides higher power densities and higher fuel burnup. Figure 17

illustrates the SFR model simulated in MCNPX 2.6.0, and Table 8 presents the reactor core's enrichment percentage and fuel mass [39, 40].

Figure 17: SFR model simulated by MCNPX 2.6.0

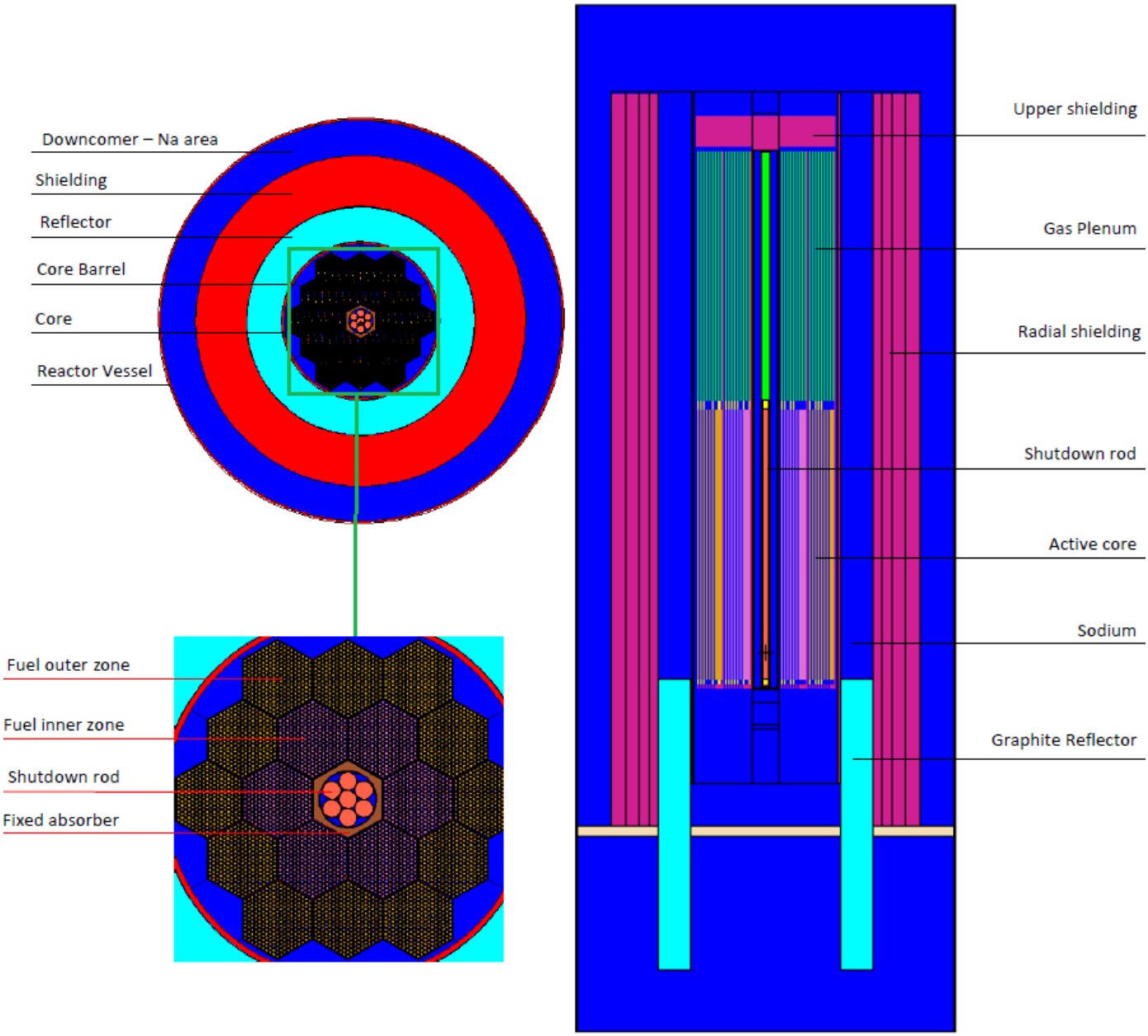

Table 8: Basic parameters of the core model

FUEL COMPOSITION	CORE REGION	
	INNER ZONE	OUTER ZONE
Number of Fuel Assembly	6	12
Initial enrichment (w/o ^{235}U)	9.20	14.60
Initial mass of uranium in FA (kg)	981.50	982.70
Initial mass of ^{235}U in FA (kg)	89.30	137.70
Initial mass of uranium by zone (kg)	5.89	11.79

The design of the fuel is based on U-10Zr (10%w Zr) binary alloy, with HT-9 steel fuel rod cladding. The graphite reflectors can move axially to allow the reactivity control, which compensates fuel burnup and reduces neutron leakage. The burnup was calculated with a standard power operation of 135 MWth and considered an extended power operation of 215 MWth. The simulation takes the prediction of cycle extension of the 10,950 equivalent full power days (EFPDs) or about 31 years for extended power, and 16,790 EFPDs or about 47 years for standard power.

Figure 18 illustrates the k_{eff} behavior during the burnup. The calculations were performed in two schemes, at the standard power of 135 MWth (Cycle 01) and another one of 215 MWth (Cycle 02) with the graphite reflector on the top of the core. Also, in the Cycle 02, the fixed absorbers are removed to allow positive core reactivity. The abrupt increase in the curve represents the EOC of Cycle 01 and the start of the BOC of Cycle 02. The k_{eff} value is 1.02775 and 1.02846 at BOC for Cycles 01 and 02, respectively. The reactor became sub-critical after 6,935 EFPDs (19 years) and 4,015 EFPDs (11 years) for Cycle 01 and Cycle 02, respectively. This results in a total of 10,950 EFPDs or 31 years of reactor operation. The k_{eff} in cycle 2 shows a curve with saw-toothed appearance between 25 to 31 years, which is caused by the computational effort to perform the calculation following changes in the fuel isotopes composition.

Figure 18: Effective multiplication factor as function of burnup

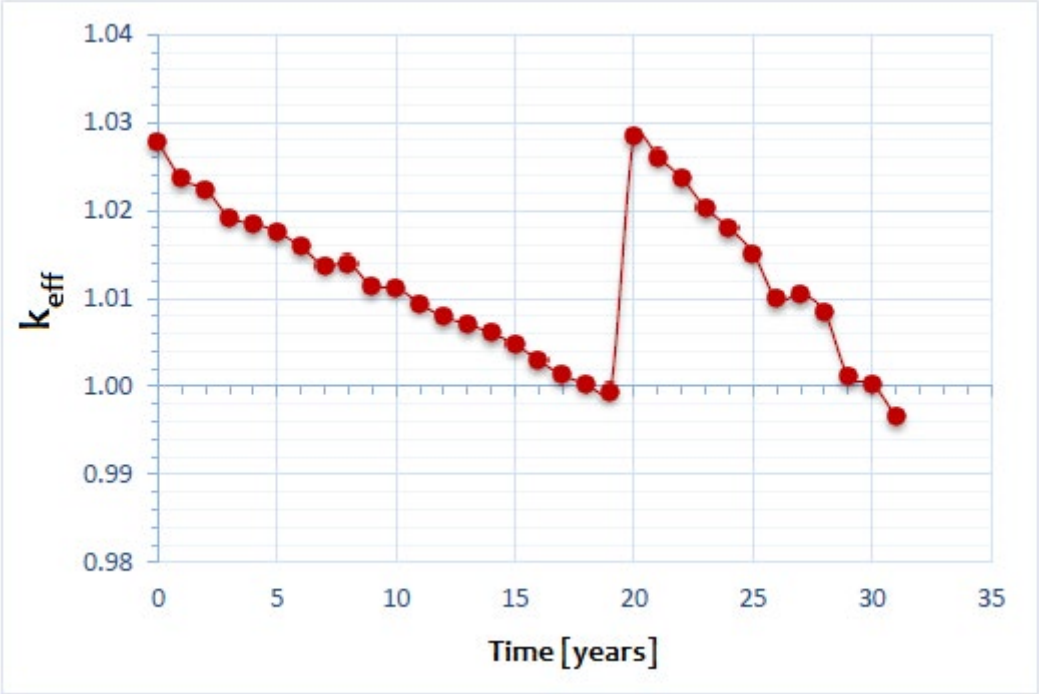

Figure 19 illustrates the initial mass of the fuel for Cycle 01 at BOC, while Figure 20 shows the mass variation between Cycle 01 at BOC and Cycle 02 at EOC. As expected, there is a mass reduction of uranium and a mass increase of ^{239}Pu after the burnup. This behavior can be due to the fission of ^{235}U and the fission and transmutation of ^{238}U to ^{239}Pu. Comparing Figure 19 and 20, the ^{235}U mass decrease is 70,9% and 75,3% for outer and inner zones, respectively. For the ^{238}U these reductions are 10,6% and 13,9%. In this way, the inner zone produces a bigger uranium reduction than the outer zone. However, the mass increase of the ^{239}Pu has an inverse behavior, that is, the outer zone presents the biggest mass of this nuclide (Figure 20). Despite ^{239}Pu production, it is possible that the inner region burns more ^{239}Pu by fission reaction than the outer zone.

Figure 19: Initial mass of the uranium for Cycle 01 at BOC

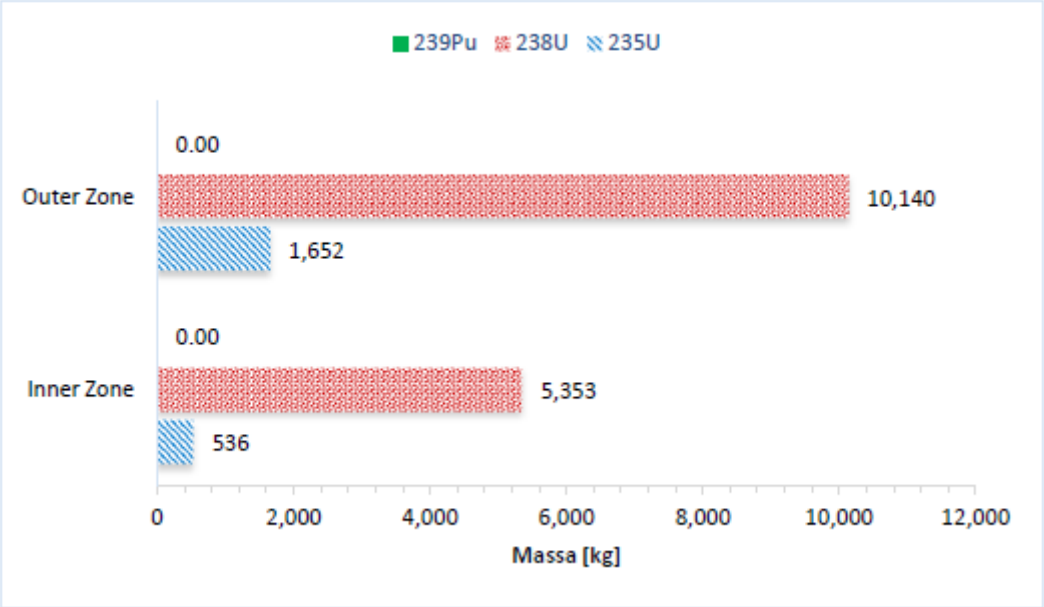

Figure 20: Mass variation between Cycle 01 (BOC) and Cycle 02 (EOC)

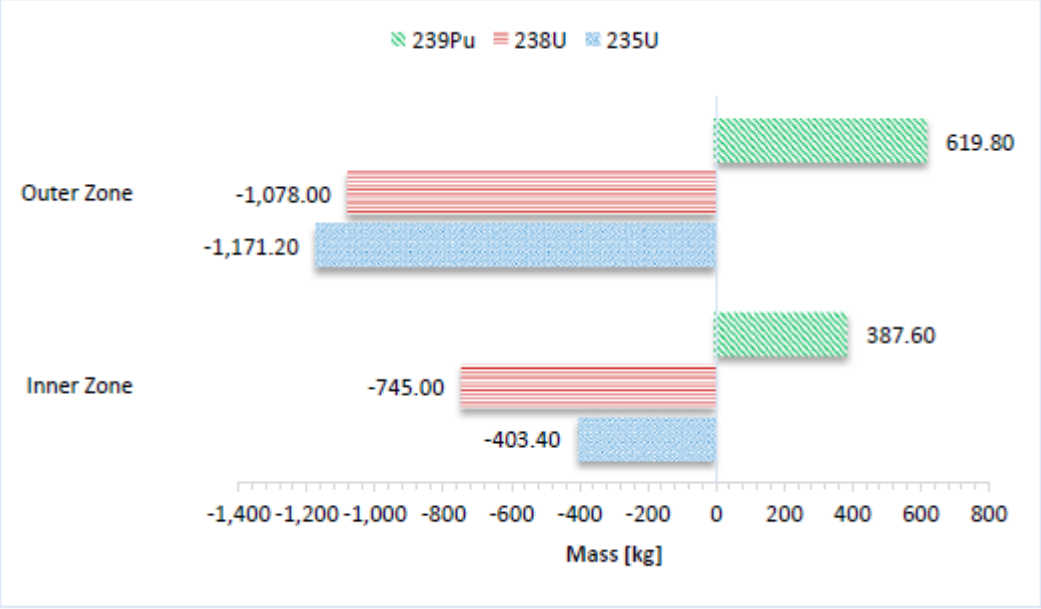

Figure 21 shows that the neutron flux in the inner zone is more significant than in other regions, as expected. This characteristic contributes to the biggest burnup of ^{235}U, ^{238}U

and ^{239}Pu. Also, the neutron flux spectrum increases to higher energy, an intrinsic characteristic of SFR.

Figure 21: Neutron flux in three different reactor zones

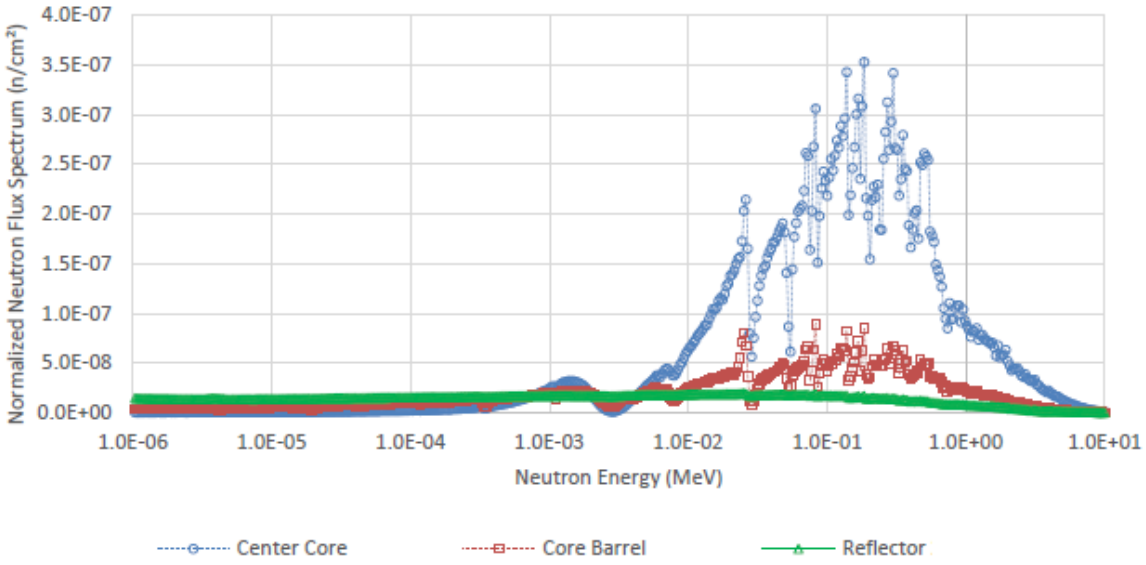

4. CONCLUSIONS

This paper presents an overview of simulations of the Fourth Generation Reactors performed by research group of DENU-UFMG. It is possible to simulate advanced reactors and verify the results using the available information of the literature. The SCALE 6.0 (KENO-VI/ORIGENS), MCNPX 2.6.0 and MCNP5 allow detailed core configuration and fuel evaluation at steady-state and/or during the burnup. The models' responses agree with expected behavior and the used codes are capable of simulating the studied reactors, which have features close to advanced systems, mainly regarding the geometry and the operational aspects. The models developed at DENU-UFMG have been updated according to the progress in research related to Fourth Generation Reactors. Currently, the models presented in this article are being configured by other neutronic and thermal hydraulic codes. Future

works will be developed to compare the results between them and to perform studies about neutronic/ thermal-hydraulic coupling studies.

In addition to scientific studies, the developed models are used for academic studies. The used codes are suitable for graduate students researching scientific calculations to master and/or doctoral thesis. Also, undergraduate students are encouraged to participate in research groups by specific projects of scientific education. All developed projects aim to produce scientific results and qualify professionals for the nuclear field. In this way, the Federal University of Minas Gerais has contributed to scientific research and the diffusion of nuclear knowledge.

ACKNOWLEDGMENT

The authors are grateful to the Brazilian research funding agencies, CNPq (Brazil), CAPES (Brazil), FAPEMIG (MG/Brazil) and CNEN (Brazil), for the support.

CONFLICT OF INTEREST

All authors declare that they have no conflicts of interest.

REFERENCES

[1] IAEA - International Atomic Energy Agency. **Nucelar Innovations for Net Zero. IAEA Bulletin, September 2023**, IAEA publications, 2023. 36p.

[2] NEA - Nuclear Energy Agency. **GEN IV International Fórum. Annual Report 2022**, OECD Publications, 2022. 84p.

[3] INCT - Instituto Nacional de Ciências e Tecnologia de Reatores Nucleares Inovadores. Brazil. 2023. Available at:

<https://estatico.cnpq.br/programas/inct/_apresentacao/inct_reatores_nucleares.html>. Last accessed: 05 Jan. 2024.

[4] CARDOSO, F; FORTINI, A.; PEREIRA, C.; COSTA, A. L.; VELOSO, M. A. F.; SILVA, C. A. M. High-Temperature Gas Reactor with Transuranic Fuels. *In*: INTERNATIONAL CONGRESS ON ADVANCES IN NUCLEAR POWER PLANTS, 2016, São Francisco. **Proceedings of International Congress on Advances in Nuclear Power Plant**, São Francisco, 2016. p. 1-7.

[5] CARDOSO, F.; PEREIRA, C.; VELOSO, M. A. F.; SILVA, C. A. M.; CUNHA, R. ; COSTA, A. L. A Neutronic Evaluation of Reprocess Fuel and Depletion Study of VHTR using MCNPX and WIMSD5 Code. **Fusion Science and Technology**, v. 61, p. 338-342, 2012.

[6] CARDOSO, F.; PEREIRA, C.; COSTA, A. L.; SILVA, C. A. M.; VELOSO, M. A. F. A Neutronic Evaluation of VHTR and LS-VHTR, *In*: 1ST INTERNATIONAL CONFERENCE ON ADVANCEMENTS IN NUCLEAR INSTRUMENTATION, MEASUREMENT METHODS AND THEIR APPLICATIONS, 2009, Marseille. **Proceedings of 1st International Conference on Advancements in Nuclear Instrumentation, Measurement Methods and their Applications**, Marseille, 2009, pp. 1-7.

[7] CARDOSO, F.; PEREIRA, C.; COSTA, A. L.; VELOSO, M. A. F. A Preliminary Neutronic Evaluation and Depletion Study Of VHTR and LS-VHTR Reactors using the Codes: WIMSD5 and MCNPX, *In*: INTERNATIONAL NUCLEAR ATLANTIC CONFERENCE, 2009, Rio de Janeiro. **Procedings of International Nuclear Atlantic Conference 2009**, Rio de Janeiro : Comissão Nacional de Energia Nuclear, 2009. p. 1-12.

[8] FORTINI, A.; MONTEIRO, F. B. A.; SCARI, M. E.; DA SILVA, F. C.; SOUZA, R. V.; SILVA, C. A. M.; COSTA, A. L.; PEREIRA, C.; VELOSO, M. A. F. Recent advances on the use of reprocessed fuels and combined thorium fuel cycles in HTR systems. **Progress in Nuclear Energy (New Series)**, v. 83, pp. 482-496, 2015.

[9] FORTINI, A.; PEREIRA, C.; SOUZA, R. V.; VELOSO, M. A. F.; COSTA, A. L.; SILVA, C. A. M. Behavior of a High Temperature Gas Reactor with Transuranic Fuels, *In*: INTERNATIONAL NUCLEAR ATLANTIC CONFERENCE, 2015, São Paulo. **Proceedings of International Nuclear Atlantic Conference**, São Paulo: Comissão Nacional de Energia Nuclear, 2015. p. 1-15.

[10] GILBERT, M.; VELASQUEZ, C. E.; VARGAS, M. L.; MARTINS, F.; COSTA, A. L.; VELOSO, M. A. F.; PEREIRA, C. Alternative Proposal of a Small Fast Sodium Reactor Concept. **Nuclear Engineering and Design**, v. 337, p. 128-140, 2018.

[11] GILBERTI, M.; VELASQUEZ, C. E,; VARGAS, M. L.; PEREIRA, F. M. G.; COSTA, A. L.; VELOSO, M. A. F.; PEREIRA, C. Analysis of a Small Fast Sodium Reactor Concept, *In*: INTERNATIONAL NUCLEAR ATLANTIC CONFERENCE, 2017, Belo Horizonte. **Proceedings of International Nuclear Atlantic Conference**, Belo Horizonte: Comissão Nacional de Energia Nuclear, 2017, p. 1-12.

[12] GUERRA, G. F.; SILVA, C. A. M; PEREIRA, C.; FERREIRA A. F. M.; COSTA, A. L.; VELOSO, M. A. F. Avaliação de Frações de Empacotamento e de Material Físsil para Combustíveis VHTR, *In*: INTERNATIONAL NUCLEAR ATLANTIC CONFERENCE, 2015, São Paulo. **Proceedings of International Nuclear Atlantic Conference**, São Paulo: Comissão Nacional de Energia Nuclear, 2015, pp. 1-8.

[13] MACEDO, A. A. P.; CASTRO, V. F.; SILVA, C. A. M.; CABRERA, C. E. V.; PEREIRA, C. Neutronic Evaluation of Transuranics in a GFR Model Using MCNPX and SCALE 6.0, *In*: INTERNATIONAL NUCLEAR ATLANTIC CONFERENCE, 2017, Belo Horizonte: **Proceedings of International Nuclear Atlantic Conference**, Belo Horizonte: Comissão Nacional de Energia Nuclear, 2017. p. 1-10.

[14] MACEDO, A. A. P.; CASTRO, V. F.; VELASQUEZ, C. E.; SILVA, C. A. M.; PEREIRA, C . Neutronic Evaluation of a GFR of 100 MWt with Reprocessed Fuel and Thorium Using SCALE 6.0 and MCNPX. *In*: INTERNATIONAL CONFERENCE ON FAST REACTORS AND RELATED FUEL CYCLES: NEXT GENERATION NUCLEAR SYSTEMS FOR SUSTAINABLE DEVELOPMENT, 2017, Yekaterinburg. **Proceedings of International Conference on Fast Reactors and Related Fuel Cycles: Next Generation Nuclear Systems for Sustainable Development**, Viena, 2017. v. IAEA. p. 1-9.

[15] MACEDO, A. A. P.; VELASQUEZ, C. E.; SILVA, C. A. M.; PEREIRA C. Neutronic Analysis of Reprocessed Fuel jn a Gas-Cooled Fast Reactor. *In*: INTERNATIONAL CONGRESS ON ADVANCES IN NUCLEAR POWER PLANTS, 2016, São Francisco. **Proceedings of International Congress on Advances in Nuclear Power Plants**, São Francisco 2016. p. 1-5.

[16] MACEDO, A. A. P.; CABRERA, C. E. V.; SILVA, C. A. M.; PEREIRA, C. Neutronic Performance of (U, Pu)C Fuel in a Lattice of GFR Using Scale 6.0., *In*: MATERIALS IN NUCLEAR SCIENCE AND TECHNOLOGY, 2015, Cancun. **Proceeding of Materials in Nuclear Science and Technology**, Cancun, 2015. p. 1-10.

[17] SALOMÉ, J. A. D.; CARDOSO, F.; VELASQUEZ, C. E.; PEREIRA, F.; BARROS, G. P.; PEREIRA, C. VHTR, ADS, and PWR Spent Nuclear Fuel Analysis. **Procedia Chemistry**, v. 21, pp. 255-262, 2016.

[18] SILVA, C. A. M.; PEREIRA, C.; COSTA, A. L.; VELOSO, M. A. F.; GUAL, M. R.; Analysis of TRISO Packing Fraction and Fissile Material to DB-MHR Using LWR Reprocessed Fuel, *In*: INTERNATIONAL NUCLEAR ATLANTIC CONFERENCE, 2013, Recife. **Proceedings of International Nuclear Atlantic Conference**, Recife: Comissão Nacional de Energia Nuclear, 2013. p. 1-12.

[19] SILVA, C. A. M.; PEREIRA, C.; VELOSO, M. A. F.; COSTA, A. L. A methodology to a DB-MHR fuel recharge evaluation - A basic comparison between WIMSD-5B and MCNPX codes. **Nuclear Engineering and Design**, v. 248, p. 117-125, 2012.

[20] SILVA, C. A. M.; PEREIRA, C.; VELOSO, M. A. F.; COSTA, A. L. Neutronic Evaluation of a MHR System to Transmutation of Minor Actinides. **IEEE Transactions on Nuclear Science**, v. 57, p. 2708-2713, 2010.

[21] SILVA, F. C.; PEREIRA, C.; VELOSO, M. A. F.; COSTA, A. L. Shifting Study of a VHTR Using Reprocessed Fuel With Various Triso Packing Fractions. **Nuclear Engineering and Design**, v. 248, p. 42-47, 2012.

[22] SOUZA, R. V.; SILVA, C. A. M.; FORTINI, A.; PEREIRA, C.; VELOSO, M. A. F.; COSTA, A. L. Neutronic Evaluation of the HTR-10 Using SCALE, MCNPX and MCNP5 Nuclear Codes, **In**: 22ND INTERNATIONAL CONFERENCE ON NUCLEAR ENGINEERING, 2014, Prague. **Proceedings of 22nd International Conference on Nuclear Engineering**, Prague, 2014. p. 1-5.

[23] SOUZA, R. V.; TANURE, L. P. A. R.; COSTA, D. F.; PEREIRA, C.; DE OLIVEIRA, A. H. A preliminary neutronic evaluation of the high temperature nuclear reactor (HTTR) using reprocessed fuel. **Annals of Nuclear Energy**, v. 65, p. 232-238, 2014.

[24] TANURE, L. P. A. R.; SOUZA, R. V.; COSTA, D. F.; CARDOSO, F.; VELOSO, M. A. F.; PEREIRA, C. A preliminary neutronic evaluation of high temperature engineering test reactor using the SCALE6 code. **Radiation Physics and Chemistry**, v. 95, p. 417-419, 2014.

[25] VARGAS, M. L.; CASTRO, V. F.; MACEDO, A. A. P.; PEREIRA, C. A Study On Plate-Type Fuel In a Generation-IV GFR. *In*: IV QUARTA SEMANA DE ENGENHARIA NUCLEAR E CIENCIAS DAS RADIAÇÕES, 2018, Belo Horizonte. **Annals of Quarta Semana de Engenharia Nuclear e Ciências das Radiações**. Belo Horizonte: Universidade Federal de Minas Gerais, 2018. p. 483-489.

[26] VIEIRA, A. L.; SILVA, C. A. M.; MAGALHÃES, I. R.; PEREIRA, C. Neutronic Evaluation of MSBR System using MCNP Code, *In*: INTERNATIONAL NUCLEAR

ATLANTIC CONFERENCE, 2019, Santos. **Proceeding of International Nuclear Atlantic Conference**, Santos: Comissão Nacional de Energia Nuclear, 2019. p. 1-10.

[27] IAEA - International Atomic Energy Agency. **Gas-cooled Reactors and their Applications. IAEA-TECDOC-436**, Vienna: IAEA, 1987, 520p.

[28] CHAPIN, D.; KIFFER, S.; NESDELL, J. **The Very High Temperature Reactor: A Technical Summary**, Alexandria: MPR Associates, Inc., 2004.

[29] CUVELIER, M. H. M.; TSVETKOV, P. V. TRU management and ^{235}U consumption minimization in fuel cycle scenarios with AP1000 and VHTRs. **Annals of Nuclear Energy**, v. 55, p.137-150, 2013.

[30] ROSENTHAL, M.W.; KASTEN, P. R.; BRIGGS, R. B. Molten Salt Reactors – History, Status, and Potential. **Nuclear Applications and Technology**, v. 8, p.107-117, 1970.

[31] ROBERTSON, R. C. **Conceptual Design Study of a Single-Fluid Molten-Salt Breeder Reactor. ORNL-4551**, USA: Oak Rigde National Laboratory,1971.

[32] RYKHLEVSKII, A.; LINDSAY, A.; HUFF, K. Full-Core Analysis of Thorium-Fueled Molten Salt Breeder Reactor Using the SERPENT 2 Monte Carlo Code, *In*: ANS ANNUAL AND WINTER MEETINGS, 2017, Washington, D. C. **Transactions of the American Nuclear Society**, Washington, D. C., 2017, v. 117, p.1343-1346.

[33] PARK, J.; JEONG, Y.; LEE, H. C.; LEE, D. Whole core analysis of molten salt breeder reactor with online fuel reprocessing. **International Journal of Energy Research**. v. 39, p. 1673-1680, 2015.

[34] VAN ROOIJEN W. F. G. Gas-cooled Fast Reactor: A Historical Overview and Future Outlook. **Science and Technology of Nuclear Installations**, v. 2009, p. 1–11, 2009.

[35] WEAVER, K. D.; TOTEMEIER, T. C.; CLARK, D. E.; FELDMAN E. E.; HOFFMAN, E. A.; VILIM, R. B.; WEI, T. Y. C.; GAN, J.; MEYER, M. K. ; GALE, W. F.; DRISCOLL, M. J.; GOLAY, M.; APOSTOLAKIS, G.; CZERWINSKI, K. **Gas-Cooled Fast Reactor (GFR) FY 05 Annual Report. Report INL/EXT-05-00799**, Idaho National Laboratory (INL), 2005.

[36] MARTÍN-DEL-CAMPO, C.; REYES-RAMÍREZ, R.; FRANÇOIS, J. L.; REIKING-CEJUDO, A. J. Contributions to the neutronic analysis of a gas-cooled fast reactor. **Annals of Nuclear Energy**, v. 38, p. 1406-141, 2011.

[37] CEA - Commissariat à l'Energie Atomique, Nuclear Energy Divison. **4th Generation Sodium-Cooled Fast Reactors – The Astrid Technological Demonstrator**, Saclay: CEA, 2012. 96p.

[38] IAEA - International Atomic Energy Agency, **Innovative small and medium sized reactors: Design features, safety approaches and R&D trends. Report IAEA-TECDOC-1451**, Vienna: IAEA, 2005. 221p.

[39] TCPSC - Toshiba Corporation Power System Company. Overview of fast reactor development of Toshiba – 4S and TRU burner, *In*: NORDIC NUCLEAR FORUM FOR GENERATION IV REACTORS, 2014, Sweden.

[40] CRIEPI - Toshiba Corporation and Central Research Institute of Electric Power Industry. **Super-Safe, Small and Simple Reactor (4S, TOSHIBA Design). ARIS Status Report AIEA**, Japan: CRIEPI, 2013. 38p.

LICENSE